



ELSEVIER

Electrically active defects due to end-of-ion-range damage in silicon irradiated with MeV Ar⁺ ions

P.K. Giri, S. Dhar, V.N. Kulkarni, Y.N. Mohapatra *

Department of Physics, Indian Institute of Technology, Kanpur 208016, India

Received 24 October 1995; revised form received 8 December 1995

Abstract

Damage induced by MeV Ar⁺ ion implantation and end of range defects in Si have been studied by capacitance–voltage, thermally stimulated capacitance, deep level transient spectroscopy (DLTS) and time analyzed transient spectroscopy (TATS). Unlike earlier studies, which focus on defects induced during post-implantation annealing steps, we study as-implanted p-type silicon samples. We report the occurrence of mid-gap acceptor levels using DLTS and TATS in a region well beyond the ion range. The presence of temperature dependent series resistance due to damaged region distorts DLTS lineshapes, even leading to sign reversal of DLTS peaks in some cases. A new and better method of correcting series resistance effects in capacitance transients has been employed. It is based on detecting the point of inversion of isothermal transients which are nonmonotonic due to the presence of series resistance. The capture process is found to be thermally activated with a high barrier energy. Possible origin of capture barrier and broadening in activation energy are discussed. Our results indicate that these deep levels are associated with point defects with local disorder in the neighbourhood.

1. Introduction

The effect of high-energy heavy ion implantation in semiconductors is being investigated extensively at present due to its potential applications in tailoring material properties and device structures [1–3]. This is primarily due to its ability to introduce deep buried layers with controlled damage and doping [2]. Specifically, argon ion implantation in semiconductors has been recognized as a means in the gettering process and it seems to be very attractive for lifetime control in silicon offering the advantage of stability with respect to annealing [4,5]. However, suitability of high energy implantation rests on a thorough understanding of dynamics of defects induced by implantation and their subsequent annealing. Damage created by heavy ion implantation has been studied by electron microscopy [6–9], Rutherford backscattering spectrometry, positron annihilation spectroscopy and infrared absorption measurements [10] from which structural information on defects are obtained. Recently, the study of point defects generated by MeV ions has assumed greater significance since identification and underlying kinetics of point defects seem to hold the key to structural relaxation [11], extended defect formation on annealing [8,12] and electrical activation of dopants [13] in the damaged layer. Traditionally, electrically active defects have been studied

by deep level transient spectroscopy (DLTS) for low doses of implantation with heavy ions [14,15]. For higher doses of implantation, use of DLTS has been mostly limited to samples annealed at high temperature in order to remove heavy disorder [16–18]. Furthermore, there has been very few studies on p-type Si compared to n-type Si. There has been hardly any study on the electrically active point defects or extended defects beyond the ion range in as-implanted samples, i.e. prior to any high temperature annealing processes. Such identification and characterization is becoming increasingly important in view of the need to understand defect creation mechanisms and dependence of defect dynamics on processing parameters.

There are several problems which need to be addressed for a meaningful electrical characterization of deep level defects in as-implanted semiconductors. Principal among them is the effect of the presence of a physically disordered region which renders invalid the standard analysis of depletion layer spectroscopy such as DLTS. There are also associated interpretational problems arising from different contributions to non-exponential nature of capacitance transients. Recently we have used an isothermal spectroscopic method to study non-exponentiality of transients and shown its advantages over traditional DLTS analysis for other standard defects in GaAlAs [19] and semi-insulating GaAs [20]. These techniques can therefore now be used for evaluating defects in implant induced semiconductors.

* Corresponding author. Tel. +91 512 257802, fax +91 512 250260 or +91 512 250007, e-mail ynm@iitk.ernet.in.

In this article, we study electrically active defects induced by MeV Ar⁺ ions in p-type silicon. The as-implanted samples are studied by capacitance–voltage (*C–V*) and thermally stimulated capacitance (TSCAP), time analyzed transient spectroscopy (TATS) and deep level transient spectroscopy (DLTS) measurements. The results point at the involvement of structural defects beyond the range of the ion. The nature of these defects are evaluated by capture and emission measurements.

2. Experimental details

Polished p-type silicon wafers of 4–7 Ω cm resistivity, (111)-orientation was used for making Schottky contact with vacuum deposited aluminium. Control diodes tested by *C–V* measurement showed uniformity of shallow doping. *I–V* measurements were done to check the quality of the diode. The implantations were performed at room temperature with 1.5 MeV Ar⁺ ions for doses of 1×10^{14} and 5×10^{14} ions/cm² on the finished device from the front side of the device. No post-implantation annealing was done on any of the samples. A Boonton capacitance meter (72B) was used for *C–V* and DLTS measurement. The whole set up is computer (PC) controlled, except for temperature control.

3. Method of series resistance analysis

In as-implanted samples, the presence of thin layer of damage created by implanted species gives rise to high series resistance. In presence of series resistance R_s in a Schottky diode, the true capacitance C_s is related to the measured capacitance C_m by

$$C_m = \frac{C_s}{(1 + \omega^2 R_s^2 C_s^2)}, \quad (1)$$

where ω is a test signal frequency of the capacitance meter.

If R_s is such that $\omega^2 R_s^2 C_s^2 > 1$, then C_m goes through a maximum when plotted with respect to time. At this point of inversion (time t_m) of the nonmonotonic transient, $\omega R_s C_s = 1$ which can be easily obtained by differentiating Eq. (1) with respect to time. So,

$$R_s = 1/\omega C_s(t_m) = 1/2\omega C_m(t_m). \quad (2)$$

Knowing R_s for a particular temperature (in case of isothermal transient) we get from Eq. (1)

$$C_s = 2C_m \frac{1 - \sqrt{1 - x^2}}{x^2} \quad \text{for } t < t_m, \quad (3)$$

$$C_s = 2C_m \frac{1 + \sqrt{1 - x^2}}{x^2} \quad \text{for } t > t_m,$$

where $x = 2\omega R_s C_m(t)$.

Thus from the actual capacitance (C_s) transient, we construct a spectroscopic signal $S(T)$ given by

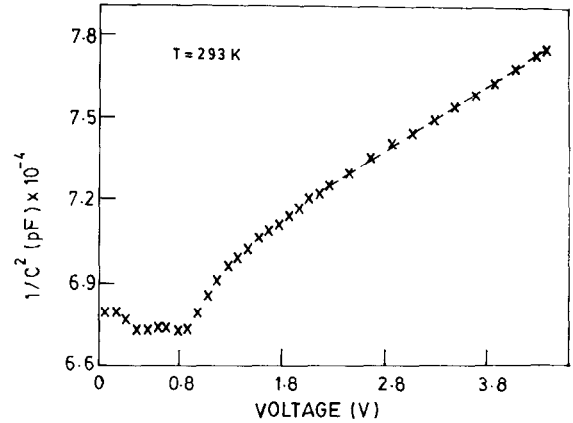


Fig. 1. $1/C^2$ vs. V_j plot for p-Si irradiated with 1.5 MeV Ar⁺ ion at dose 1×10^{14} ions/cm². The dotted line is the least square fit giving shallow acceptor concentration.

$$S(T) = C_s(t, T) - C_s((1 + \gamma)t, T), \quad (4)$$

γ is a experimentally chosen constant. This is known as a TATS signal [19]. Being an isothermal spectroscopic technique it has many advantages over other conventional spectroscopic techniques such as DLTS and temperature scanning techniques [19,20]. When plotted against the logarithm of time, $S(T)$ goes through a maximum at time t_m given by

$$e_n = \frac{\ln(1 + \gamma)}{\gamma t_m}, \quad (5)$$

where e_n is the emission rate of the trap level.

From the Arrhenius plot corrected time constants are obtained.

4. Results and discussion

In order to see the degree of damage created by implanted ion species (Ar⁺), *C–V* measurements were done on the control sample and the implanted sample with two different doses (a) 1×10^{14} and (b) 5×10^{14} ions/cm². In contrast to the control sample, the irradiated sample with dose 1×10^{14} ions/cm² shows a flat region in the $1/C^2$ vs. V plot indicating the presence of a damaged region which increases with increasing dose (see Fig. 1). The dose of 5×10^{14} ions/cm² is close to the amorphization dose. This is in good agreement with the results of Bollmann et al. [21]. Beyond the damaged region, both the control and irradiated sample show an identical shallow level profile. Thus the $1/C^2$ method allows the determination of the extent of the damaged region. *C–V* measurements at lower temperatures showed partial carrier freeze out resulting in a temperature dependent series resistance in the device.

The control sample is tested for the presence of deep levels using DLTS. No signal was observed showing absence of deep levels up to the detection limit of 10^{11} cm⁻³. The sample irradiated with a dose of 1×10^{14} ions/cm² showed

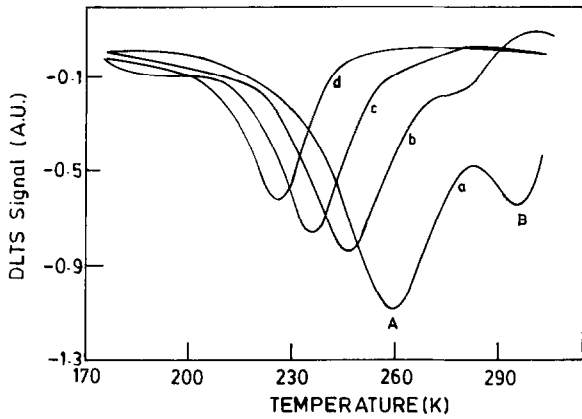


Fig. 2. DLTS spectra for Ar⁺ implanted p-Si. Rate windows: (a) 2128 s⁻¹, (b) 495 s⁻¹, (c) 125 s⁻¹ and (d) 33 s⁻¹.

a DLTS signal with two distinct peaks as shown in Fig. 2. The activation energies of the two traps as obtained from DLTS analysis are 0.60 eV and 0.62 eV for peaks labeled A and B in Fig. 2 and the corresponding Arrhenius plot for the dominant peak is shown in Fig. 3. Results from TSCAP studies also show two dominant trap levels as shown in Fig. 4.

The decrease of DLTS peak height with a decreasing rate window, as can be seen in Fig. 2, is partly due to the effect of series resistance which increases on lowering the temperature and also due to the temperature dependent occupancy of the traps for the same filling pulse. For smaller rate windows, the DLTS signal undergoes sign reversal, an effect known to occur in the presence of series resistance [22]. The methods for overcoming problems due to series resistance proposed earlier by various workers are rather cumbersome and difficult to implement in actual measurements since both resistance and capacitance are temperature dependent. The use of an external series resistance to overcome the problem, as suggested by Broniatowski et al. [22], is less practical. Moreover, the procedure is not valid for high

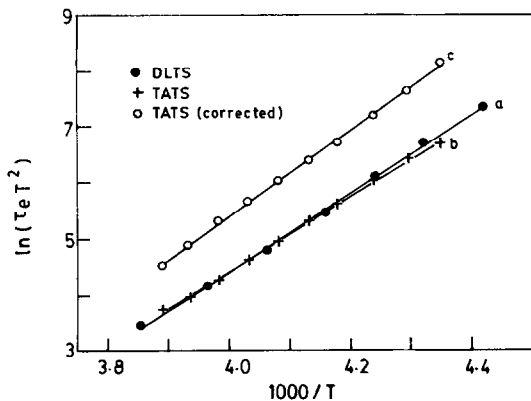


Fig. 3. An Arrhenius plot of (a) DLTS data for level A in Fig. 2, (b) TATS (without resistance correction) and (c) TATS (with resistance correction).

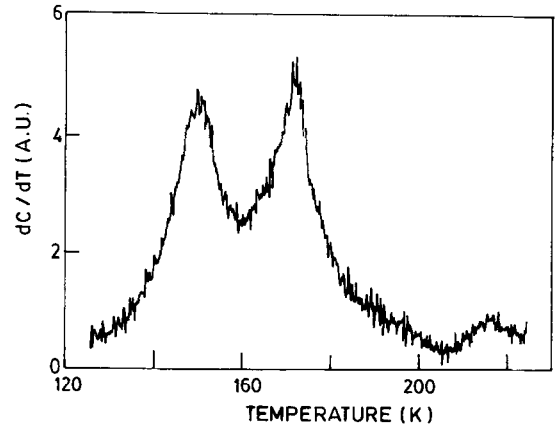


Fig. 4. Differentiated thermally stimulated capacitance (TSCAP) signal showing two major peaks. The heating rate is 2.5 K/min.

trap concentrations. The use of a low modulation frequency capacitance meter in DLTS instruments [23] severely restricts the range of usable time constants. Therefore we use TATS so that each isothermal transient can be corrected for prior to analysis, as discussed in Section 3. The estimated series resistance ranges from 2 kΩ to 3 kΩ in the temperature range 220–260 K. An Arrhenius plot of the corrected time constant is shown in Fig. 3 along with Arrhenius of DLTS data points and time constant obtained from TATS measurements using uncorrected transients. A clear distinction between corrected TATS and uncorrected TATS/DLTS data points can be seen in Fig. 3. An Arrhenius plot of time constants without resistance correction gives an activation energy (E_T) of 0.57 eV and with proper correction it is 0.66 eV. Hence, also note that activation energy obtained from DLTS measurements can be misleading due to the presence of temperature dependent series resistance.

In Fig. 5, experimental DLTS curve is compared with a simulated DLTS fitted with same time constant as that found from the experiment. The dominant peak in DLTS is broader than the corresponding exponential transients. In the pres-

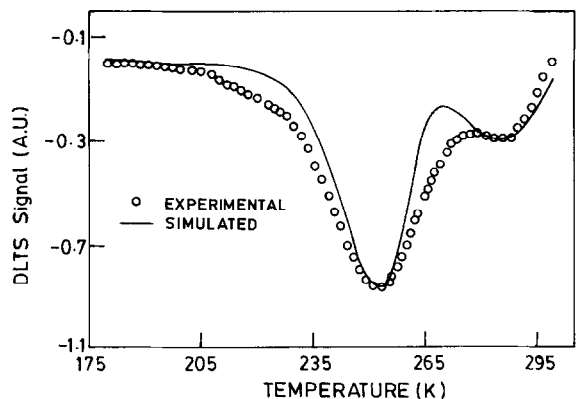


Fig. 5. Comparison of simulated and experimental DLTS spectra ($\tau = 1$ ms) demonstrating broadening. Fitting is done with two exponentials.

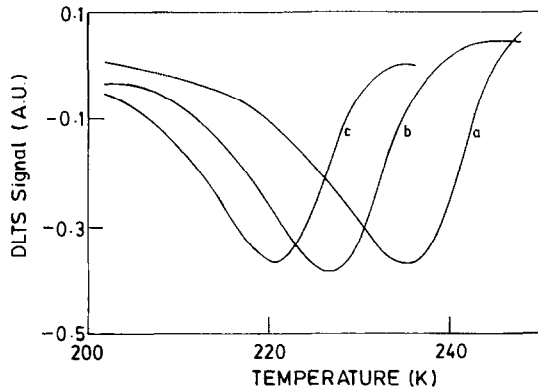


Fig. 6. Capture DLTS spectra for the same sample with rate windows: (a) 500 s^{-1} , (b) 125 s^{-1} (c), 50 s^{-1} .

ence of a series resistance, the DLTS peak height is known to get reduced. It can also be shown easily from simulation that the DLTS line width is reduced due to series resistance and its peak position is shifted towards higher temperatures for the same rate window [24]. So, a proper estimation of broadening in DLTS lineshape is not possible as the resistance is temperature dependent and it distorts the DLTS lineshape. The occurrence of broadening in DLTS spectra can be attributed to the spread of activation energies in the presence of inhomogeneous environment in the damaged region. Since such deep levels would experience a different strain field as in the case of less perfect crystals, the model for broadened deep energy levels would be applicable. Assuming a Gaussian distribution of energy, using all other parameters from the experiment, the observed major peak is fitted to obtain full width half maximum (FWHM) of the distribution. For the resistance corrected isothermal transients we find FWHM to be 45 meV whereas it is 30 meV for the uncorrected transients. Similar broadening of point defect energies have been obtained for deep levels found in plastically deformed silicon [25]. Leakage current effect on the DLTS spectra is negligible for the diodes studied as $nc_n \ll e_n$ for a particular temperature.

The capacitance transients during capture is observed to be surprisingly slow. Capture transients are recorded at various temperatures and analysis shows that they are exponential in nature. As suggested by Ghosh et al. [26], for a straightforward measurement of the capture barrier, DLTS scans using capture transients were taken in the temperature interval of 175–300 K. Typical capture DLTS peaks for different rate windows are shown in Fig. 6. Capture time constants have been obtained by both DLTS and TATS processing of capture transients and have been plotted in an Arrhenius plot in Fig. 7 yielding an activation energy of 0.64 eV. Note that this is an unusually high activation energy for capture processes. Since hole freeze out has been observed in the same temperature range from $C-V$ measurements, this activation energy must be the sum of the capture barrier and the equilibrium energy difference between traps and the valence band. The later energy has been estimated

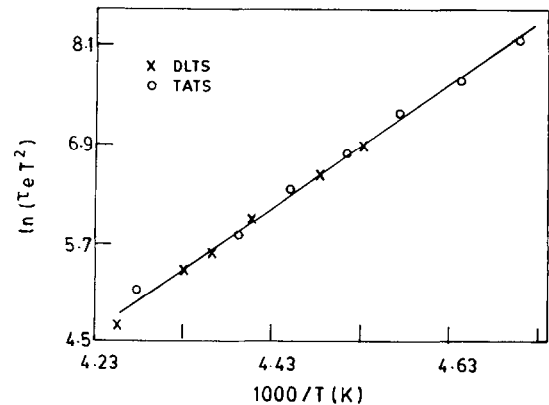


Fig. 7. Arrhenius plot obtained by DLTS and TATS analysis of capture transients.

to be 0.31 eV from $C-V$ measurement in this temperature range. Hence, the capture barrier is only 0.33 eV. Since the emission energy was found to be 0.66 eV, the ground state energy of the dominant trap is evaluated to be 0.33 eV. This indicates that there is a large lattice relaxation at these defect sites. An independent evaluation of the capture barrier by varying filling pulse-width techniques can be used to verify this energy scheme.

Since argon is known to be electrically inactive in silicon, the trapping behavior is attributed to damages created by high energy ions. The structural defects created by high-dose Ar^+ implantation [5] are: (i) dangling bonds along dislocation lines, (ii) cottrell atmosphere around the dislocations, (iii) dissolved Ar atoms, and (iv) bubbles of Ar gas. It is not clear which of these four different types of defects are responsible for the lifetime degradation process in Ar^+ implanted silicon. In our case, since the samples were not subjected to any post-implantation annealing, the traps observed beyond the ion range can be attributed to electrically active point defects with local disorder in their immediate neighbourhood. Hence the observed capture barrier is most probably due to band bending in the vicinity of the defect. Similar models of capture barriers have been invoked in plastically deformed silicon containing dislocations. However in contrast to our results, the capture barriers associated with dislocations show time dependence owing to the many electron nature of the sites. More detailed investigations on capture kinetics are under study.

5. Conclusions

In summary, we have characterized electrically active defects in Ar^+ implanted p-type silicon beyond the ion range. The damage profile due to high dose implantation is estimated by $C-V$ measurements. The tail region of the damaged region shows the signature of the energy broadened point defects. Unlike earlier studies on defects induced during post-implantation annealing steps [17], we report on

the occurrence of the acceptor levels in as-implanted silicon samples. For the dominant trap the emission energy, the capture barrier and the ground state energy has been obtained. The detailed structure and thermal stability of such defects need to be further studied in order to understand the formation mechanism of such defects and role played by them in device structures.

References

- [1] S. Kalbitzer, Nucl. Instr. and Meth. B 63 (1992) 1.
- [2] A. Golanski, Appl. Surf. Sci. 43 (1989) 200.
- [3] J.F. Ziegler, Nucl. Instr. and Meth. B 6 (1985) 270.
- [4] M. Wilander, J. Appl. Phys. 56 (1984) 3006.
- [5] H.F. Kappert, G. Sixt and G. H. Schwutke, Phys. Status. Solidi A 52 (1979) 463.
- [6] A. Claverie, C. Vieu, J. Faure and J. Beauvillain, J. Appl. Phys. 64 (1988) 4415.
- [7] K.S. Jones, S. Prussin and E.R. Weber, Appl. Phys. A 45 (1988) 1.
- [8] J.R. Liefting, J.S. Custer and F.W. Saris, Mater. Sci. Eng. B 25 (1994) 60.
- [9] M. Tamura, N. Natsuaki, Y. Wada and E. Mitani, Nucl. Instr. and Meth. B 21 (1987) 438.
- [10] P.J. Simpson, M. Vos, I.V. Mitchell, C. Wu, and P.J. Schultz, Phys. Rev. B 44 (1991) 12180.
- [11] S. Roorda, S. Doorn, W.C. Sinke, P.M.L.O. Scholte and E. van Loenen, Phys. Rev. Lett. 62 (1989) 1880.
- [12] R.J. Schreutelkamp, J.S. Custer, J.R. Liefting, F.W. Saris, W.X. Lu, B.X. Zhang and Z.L. Wang, Nucl. Instr. and Meth. B 62 (1992) 372.
- [13] M. Tamura, T. Ando and K. Ohyu, Nucl. Instr. and Meth. B 59/60 (1991) 572.
- [14] B.G. Svensson, C. Jagdish and J.S. Williams, Nucl. Instr. and Meth. B 80/81 (1993) 583.
- [15] B.G. Svensson, C. Jagdish and J.S. Williams, Phys. Rev. Lett. 71 (1993) 1860.
- [16] P. Kringhoi, J.S. Williams and C. Jagdish, Appl. Phys. Lett. 65 (1994) 2208.
- [17] S. Hahn, T. Hara, T. Maekawa, N. Satoh, Y.-K. Kwon, K.-I. Kim, Y.-H. Bae, W.-J. Chung, E.K. McIntyre, W.L. Smith, L. Larson and R. Meinecke, Nucl. Instr. and Meth. B 74 (1993) 275.
- [18] C. Christofiedes, Semicond. Sci. Technol. 7 (1992) 1283.
- [19] S. Agarwal, Y.N. Mohapatra, V.A. Singh and R. Sharan, J. Appl. Phys. 77 (1995) 5725.
- [20] P.K. Giri and Y.N. Mohapatra, J. Appl. Phys. 78 (1995) 262.
- [21] J. Bollmann and H.A. Klose, Solid State Phenomena, Vol. 6 and 7 (1989) p. 461.
- [22] A. Broniatowski, A. Blossie, P.C. Srivastava and J.C. Bourgoin, J. Appl. Phys. 54 (1983) 2907.
- [23] S. Anand, S. Subramaniam and B.M. Arora, J. Appl. Phys. 72 (1992) 3535.
- [24] P.K. Giri and Y.N. Mohapatra, unpublished.
- [25] P. Omling, E.R. Weber, L. Montelius, H. Alexander and J. Michel, Phys. Rev. B 32 (1985) 6571; C. Kisielowski and E. R. Weber, Phys. Rev. B 44 (1991) 1600.
- [26] S. Ghosh and V. Kumar, J. Appl. Phys. 75 (1994) 8243(L).